



Full Length Article

Multi-stage hydrothermal liquefaction modeling of sludge and microalgae biomass to increase bio-oil yield

Bhawna Bisht^{a,1}, Prateek Gururani^{b,1}, Shivam Pandey^c, Krishna Kumar Jaiswal^d, Sanjay Kumar^a, Mikhail S. Vlaskin^e, Monu Verma^f, Hyunook Kim^f, Vinod Kumar^{a,g,*}

^a Algal Research and Bioenergy Laboratory, Department of Life Sciences, Graphic Era (Deemed to be University), Dehradun, Uttarakhand 248002, India

^b Department of Biotechnology, Graphic Era (Deemed to be University), Dehradun, Uttarakhand 248002, India

^c Department of Chemistry, Uttarakhand University, Dehradun 248007, India

^d Department of Green Energy Technology, Pondicherry University, Puducherry 605014, India

^e Joint Institute for High Temperatures of the Russian Academy of Sciences, 13/2 Izhorskaya St, Moscow 125412, Russia

^f Water-Energy Nexus Laboratory, Department of Environmental Engineering, University of Seoul, Seoul 02504, Republic of Korea

^g Peoples' Friendship University of Russia (RUDN University), Moscow 117198, Russian Federation



ARTICLE INFO

Keywords:

Hydrothermal liquefaction
Sludge
Microalgae
Chlorella sorokiniana
Co-HTL

ABSTRACT

This study aims to elucidate the effect of Multi-Stage HTL with a constant resident time of 30 min for three different feedstocks including kitchen wastewater sludge (KwWs), freshwater microalgae *Chlorella sorokiniana* (UUIND6), Co-HTL (KwWs + UUIND6) to obtain the maximum bio-oil yield. According to the results obtained, KwWs appears to be the most suitable for conversion into energy-dense bio-oil under a sustainable biorefinery approach for increased bio-oil yields i.e., 72.75 ± 0.37 wt%, with HHV of 40.52 MJ/kg and energy recovery of 53.64 wt%. Further, the bio-oils and bio-chars derived from different types of biomasses obtained at different temperature conditions were analyzed by GC-MS, NMR, FTIR, and Raman spectroscopy to identify variations in the bio-crude compounds.

1. Introduction

Both global energy crisis as well as discharge of massive amounts of domestic effluents into sewer networks because of expanding urbanization and industrial intensification, pose significant barriers to sustainable development in the 21st century [1–3]. On the one hand, energy consumption is increasing by 2% per year as a result of fast population expansion, which is predicted to reach 9 billion by 2050 [4], which is expected to rise by 50% in the future years [3]. On the other hand, sewage sludge transports a diverse range of solid contaminants such as massive amount of organic matter like lipids (6–35%), carbohydrates (8–15%), proteins (20–30%), inorganic compounds, pathogens, heavy metals, toxic and noxious substances suspended in an impure water continuum [3,5]. Conventional sewage sludge disposal technologies (land-filling, incineration, combustion) and certain potential thermochemical processes (pyrolysis and gasification) exist for managing, treating, disposing, and reusing sludge waste. However, these pathways

confront substantial obstacles such as high costs, secondary pollution, deprecation of critical resources (land, energy, labour), health concerns, stringent legal policies, and the need to stabilize the physical nature of sewage sludge, which is especially difficult with wet sewage sludge [6].

Despite the growing environmental sustainability concerns associated with rising CO₂ emissions and sewage sludge, the scientific community has been challenged in recent decades to realign the path toward a 100% renewable energy system capable of addressing both the rising challenges of energy security as well as sludge disposal in a simple and effective manner [7]. This sophisticated procedure utilizes a variety of major benefits of using alternative energy sources to address environmental challenges related with the usage of fossil fuels and sludge and bridge the gap of their depletion and accumulation, respectively [8].

Municipal sewage sludge biomass is regarded as one of the most promising alternatives to fossil fuels since it fits all the conditions for renewable and CO₂-neutral materials while also being one of the world's greatest energy sources [9]. Aside from direct energy generation, there

* Corresponding author at: Algal Research and Bioenergy Laboratory, Department of Life Sciences, Graphic Era (Deemed to be University), Dehradun, Uttarakhand 248002, India.

E-mail address: vinodkhatwalia@gmail.com (V. Kumar).

¹ Equal Contribution.

is considerable interest in turning biomass into more lucrative bio-products such as bio-oil, bio-chemicals, bioelectricity, and bio-syngas [10].

The European Union issued the Renewable Energy Directive to set goals for the share of renewable energy in the transport sector: a minimum of 14% of final energy consumption for transportation issues should be considered renewable by 2030, with 3.5% of that provided by advanced biofuels produced from specific biomass such as algae or biomass fractions [11]. The Energy Efficiency and Renewable Energy (EERE) Bioenergy Technology Office (BETO), United States Energy Department Office, is also functioning to promote the adoption of technological innovations that can transform gaseous and wet renewable biomass into high-performance biofuels compatible with modern transportation infrastructure [12].

In light of rising environmental concerns and new waste management challenges, HTL is one among the eminent developing technologies that is becoming increasingly popular nowadays in expanding waste-to-energy conversion potentialities on the far side generating heat and electricity [13,14]. The high molecular weight organic biomass is primarily depolymerized during this HTL process, and small organic compounds with reactive properties combine to form new compounds, namely bio-oil or bio-crude, gas residue, aqueous phase, and solid residue, as a result of various polymerization reactions such as hydrolysis, deoxygenation, repolymerization, fragmentation, aromatization, and dehydration [15]. The basic idea behind HTL process is to understand the advantages of chemical and physical interactions between targeted reactants and solvent molecules, such as improved solvation ability and molecular properties like ionic product and dielectric strength change to increase the extraction of specific organic components like carbohydrates, gases, proteins, and fatty acids. Furthermore, it is categorized based on operating temperature into hydrothermal gasification, hydrothermal liquefaction, and hydrothermal carbonation [16]. The growing trend of sustainable biofuel generation through HTL process is particularly interesting that can treat wet/dry feedstock biomass, starting from lignocellulosic to algae to sludge wastes, into an energy-dense bio-oil which will be upgraded and fractionated to varied liquid biofuels such as kerosene, diesel, and petrol [17-19], for instance, KwWs is readily available in large volumes and unlike bioenergy feedstocks such as microalgae, does not require cultivation. The use of such wet sludge waste to produce biofuel in transportation may considerably cut back 1) Disposal of non-beneficial sludge; 2) CO & total hydrocarbon emissions, and particulate matter; 3) residual waste management cost making the process safer, less hazardous and more biodegradable [12]. Previous work also reported that sludge is amenable to HTL treatment for biofuel production ranging from 10 to 45 wt% for HTL temperatures ranging from 523 to 673 K, but availability and compositions are prone to seasonal and local fluctuations. Additionally, to providing feedstock for biofuel, Co-HTL of sewage waste results in the removal of considerable heavy metals and weakly bio-degradable toxic chemicals, which are subsequently converted to bio-char residues and employed in a number of bio-refinery applications [20,21]. A number of research have recently been carried out to gain the harmlessness, reduction, and aid usage of sewage sludge using HTL process for instance, Co-HTL of various waste-derived feedstock and microalgal biomass has confirmed more bio-oil production in addition to improved fuel properties [22-24]. Another study found ~ 40 % bio-oil yield and progressed electricity restoration with excessive ester concentration on co-liquefaction of microalgae and sweet potato waste (4:1 wt%) [25]. However, primarily based on the above research, there are few challenges that obstruct bio-oil yield from sewage sludge such as existence of a complicated biochemical composition, high mineral content and low volatile matter [26].

Unlike the sludge, the use of microalgae has lately acquired traction among researchers as a means to improve treatment efficiency and reuse sludge in order to lessen environmental and financial constraints. They have a unique potential to deliver ecological services while also responding to the sustainability challenges, allowing them to reap

multifaceted benefits and reinforce the goals of resource efficient bio-economy. Microalga UUIND6 HTL research for sustainable biofuel production has grown in popularity in recent decades due to their fast growth rate, higher photosynthetic efficiency, ability to accumulate a high lipid content, and high applicability to non-arable land environments when compared to terrestrial lignocellulosic plants [27]. Furthermore, they can be grown on CO₂ from industrial off-gas, resulting in a partially closed carbon cycle. Algal biofuel yields can reach up to 40–50%, however the quality is highly dependent on the algae strain used.

There has been no comprehensive investigation on the effects of different temperature conditions on all products of Multi-Stage HTL employing KwWs, freshwater green microalga UUIND6 and Co-HTL as feedstock biomasses till date. Co-HTL of distinct microalgae and sludge mixtures may be a way to combine the positive aspects of both material groups in order to expand the available data base and improve feedstock blending for future large-scale production i.e., microalgae may greatly balance the heterogeneous qualities of sludge residues while the residues increase the amount of input materials available for biofuel generation via HTL.

However, the properties of the bio-oil derived from different biomass sources of different compositions react differently under different conditions, causing different chemical reactions to produce different molecular products. Thus, the present study systematically evaluated the influence Multi-Stage HTL with different feedstock, namely KwWs, UUIND6, and Co-HTL at constant residence time of 30 min and thoroughly assessed bio-oil characteristics (bio-crude yield, elemental composition, heating value, energy recovery, conversion rate) and chemical composition and functional group. Further, the bio-oils and bio-chars derived from different types of biomasses at the same time and temperature conditions were analyzed by GC-MS, NMR, FTIR, and Raman spectroscopy to identify variations in the compounds.

2. Materials and methods

2.1. Materials

The raw feedstock biomass samples used in this study were KwWs, freshwater green microalgae (UUIND6: GenBank accession number: KY780616) were used for Multi-Stage HTL or Co-HTL process. Our research group previously isolated this microalga from a wastewater source capable of producing bio-oil [28]. KwWs was collected from the hostel mess wastewater tank located at Graphic Era deemed to be University, Dehradun, India. The sludge was rich in residues of bread, rice and vegetables etc. The collected KwWs were mechanically concentrated and dewatered without any stabilising treatment. The dewatered sludge was dried for 24 h in a hot air oven at 105C before being pulverized and screened into particle fractions. All of the chemicals and reagents used in this investigation were analytical reagent grade and obtained from HiMedia Laboratories Pvt. Ltd. in India.

2.2. Multi-Stage HTL set up and bio-crude separation procedure

Multi-Stage HTL experiments of dried KwWs, UUIND6, and Co-HTL were conducted in a custom designed stainless-steel reactor (SS-316) with a 40 ml capacity in batch mode at 3 different specified temperature ranges i.e., 250 °C (Stage-I), 350 °C (Stage-II) and 450 °C (Stage-III) with a holding time of 30 min with minor modification given by Kumar et al., [3]. Initially, the reactors were heated at the desired temperature rate (i.e., 5C/min). With regard to its reaction temperature, the reaction pressure was not regulated and was kept as auto-generated. In each test run, a fixed amount of dried feedstock biomass (4 g) was mixed with a fixed amount of water (40 ml) for the same residence duration (30 min) and loaded into the reactor for investigation of bio-oil and bio-char production.

In the Stage-I of Multi-Stage HTL process, 4 g of individual feedstock

biomass (KwWs, UUIND6, and Co-HTL) was fed with 40 ml of water i.e., in the ratio of 1:10 (biomass:water) into the reactor. Then, the reactor was sealed and heated and the reaction was carried out at 250 °C where it was maintained for 30 min. After completion of the reaction, the reactor was cooled and opened to vent off the gaseous phase. The gaseous products were not analyzed in this study since our main interests were in the solid and liquid products. Following that, dichloromethane (DCM) was used as a solvent in the reactor to extract the organic components for liquid and acetone solvent was used for solid phases. The resulting suspension was vacuum-filtered through Whatman filter paper 42. The resultant solid residue was washed with acetone many times (at least 3–4 times) to recover any leftover biocrude. The separated solid phase was known as ‘bio-char,’ and it was dried overnight in a hot air oven at 105 °C to produce dry bio-char. After this, filtrate solvents were recovered by rotary evaporator to obtain the yield (DCM + Acetone) of Bio-oil which was quantified gravimetrically. Equation (7) and (8) were used to compute the yield of bio-oil and bio-char. The bio-crude oil samples were kept at – 20 °C for further examination while bio-char samples were further used as feedstock for Stage-II of HTL. The individual dried bio-char (KwWs, UUIND6, and Co-HTL) produced in step first was again processed at 350 °C for 30 min in the second phase of Multi-Stage HTL to obtain the individual bio-oil and bio-char of KwWs, UUIND6, and Co-HTL. In the Stage-III of the, a similar approach was used with each bio-char produced in the second phase, and the experiment was carried out at 450 °C with the same holding duration. The overall bio-oil and bio-char yields were determined using Equation (11) and (12). Stage HTL of three biomass was also performed at the same temperature range, but corresponding to three different residence times (30 min, 60 min, and 90 min) to determine the effect of residence time.

2.3. Characterization of the HTL products

2.3.1. Elemental composition analysis

The elemental composition (C, H, and N) of different biomasses and derived bio-oils and bio-chars from KwWs, UUIND6 and Co-HTL were analyzed using an elemental analyzer (Thermo Fisher).

2.3.2. ^1H NMR analysis

The bio-oil profile of KwWs, UUIND6, and Co-HTL derived from Multi-Stage HTL was evaluated using ^1H NMR. Briefly, 100 mg of crude oil was combined with deuterated chloroform (550 μL), and spectra were acquired using 500 MHz NMR. The NMR spectra were processed using MestReNova the chemical shifts were further integrated based on previously published studies [29,30].

2.3.3. GC–MS analysis

The chemical composition of extracted bio-oil of KwWs, UUIND6, and Co-HTL derived from Multi-Stage HTL was investigated using gas chromatography–mass spectrometry (GC–MS) (450-GC, 240-MS, Varian, USA) with minor modification given by Arora et al. [31]. The GC–MS was outfitted with an Agilent VF-5 ms column and helium was used as the carrier gas at a flow rate of 1 ml/min. Before injection, the bio-oil was diluted 100 times in DCM and filtered via 0.2 μm PTFE membrane filters. At a split ratio of 1:10, an injection volume of 1 μL was employed and the injector temperature was kept at 300 °C. The temperature of the column was set at 80 °C for 2 min, then ramped up at a rate of 8 °C/min to 140 °C, and then for 2 min at 4 °C/min to 280 °C. The mass spectrometer was configured to a scan range of 50 to 1000 m/z with an ionizing voltage of 70 eV. The chemicals were identified by comparing the samples’ spectra to the electron impact mass spectrum from the NIST Database.

2.3.4. Raman spectroscopy analysis

The Raman spectra of different biomasses and derived bio-chars were prepared under the condition reported by Xu et al. [32]. Before

performing Raman analysis, all samples of biomass and bio-chars collected during the Multi-Stage HTL process at various temperature settings were dried for 24 h at 105C to eliminate moisture. Raman spectra were collected using a micro-Raman spectrometer.

2.4. Calculation methods

All multi-stage HTL experiments were carried out in triplicates for all three approaches under the stated circumstances to ensure reproducibility of the results and quantified using the following equations mentioned in Mishra and Mohanty [26] and Islam et al. [33].

The oxygen content was determined using the equation (1):

$$O(\%) = 100\% - (C + H + N)\% \quad (1)$$

The molar ratio of H/C, N/C and O/C were calculated from the weight percentage of C, N, H and O by using the Equations (2–4):

$$\frac{H}{C} = \frac{H \times 12.001}{C \times 1.008} \quad (2)$$

$$\frac{O}{C} = \frac{O \times 12.001}{C \times 15.999} \quad (3)$$

$$\frac{N}{C} = \frac{N \times 12.001}{C \times 14.007} \quad (4)$$

HHVs (MJ/kg) via the Dulong formula and energy recovery of the biocrudes were calculated Equation (5 and 6):

$$HHV(\text{MJ/kg}) = 0.3383C + 1.422(H - O/8) \quad (5)$$

$$\text{Energy recovery}(\%) = \text{Biocrude yield} \times \frac{HHV_{\text{of Biocrude}}}{HHV_{\text{of Feedstock Biomass}}} \quad (6)$$

Yields of bio-oil, bio-char and biomass conversion were all expressed in wt.% and calculated using the Equations (7–9). All the findings presented as mean \pm S.D values on a dry basis of feedstock.

$$\text{Biooil yield}(\text{wt.}\%) = \frac{W_{\text{dbo}}}{W_{\text{Bm}}} \times 100 \quad (7)$$

$$\text{Biocharyield}(\text{wt.}\%) = \frac{W_{\text{dbc}}}{W_{\text{Bm}}} \times 100 \quad (8)$$

$$\text{Conversion rate}(\%) = \left(1 - \frac{\text{Weight of dry bio-oil}}{\text{Weight of biomass}}\right) \times 100 \quad (9)$$

where W_{dbo} , W_{dbc} and W_{Bm} are the weight of dry bio-crude oil, dry bio-crude char and biomass sample, respectively.

Water and gaseous by-products of the Multi-Stage HTL process were not measured. The total production of water + gas (wt.%) was calculated using difference Equation (10), assuming a negligible mass loss for the liquefaction solvent during the liquefaction process.

$$\text{Total water} + \text{Gas yield}(\text{wt.}\%) = 100(\text{wt.}\%) - \text{Bio-oil}(\text{wt.}\%) - \text{Bio-char}(\text{wt.}\%) \quad (10)$$

After completion of the Multi-Stage HTL process, the overall bio-oil and bio-char yields were expressed using the following Equation (11 and 12):

$$\text{Total Biooil yield}(\text{wt.}\%) = \text{Biooil}_{250^\circ\text{C}} + \text{Biooil}_{350^\circ\text{C}} + \text{Biooil}_{450^\circ\text{C}} \quad (11)$$

$$\text{Total Biochar yield}(\text{wt.}\%) = \text{Biochar}_{250^\circ\text{C}} + \text{Biochar}_{350^\circ\text{C}} + \text{Biochar}_{450^\circ\text{C}} \quad (12)$$

2.5. Statistical data analysis

Data analysis of Multi-Stage HTL of KwWs, UUIND6 and Co-HTL experiments were carried out in triplicates. The variability of the data was displayed as mean \pm standard deviation with $p \leq 0.05$ was considered significant using OPSTAT. One way ANOVA was applied to determine the significant yield of bio-oil.

3. Results and discussion

The peculiar composition of different biomass has been found to be a paramount parameter in the HTL treatment process, making HTL reactions strikingly remarkable. Even when indistinguishable reaction conditions are constrained, this uniqueness is likewise reflected in the properties of the yielded products, which gigantically incline toward the kind of feedstock biomass exploited [34]. However, the only thing they all share practically is that they are composed of similar elements i.e., carbon, nitrogen, hydrogen, oxygen, and sulphur.

Among the various types of available biomass and waste that have

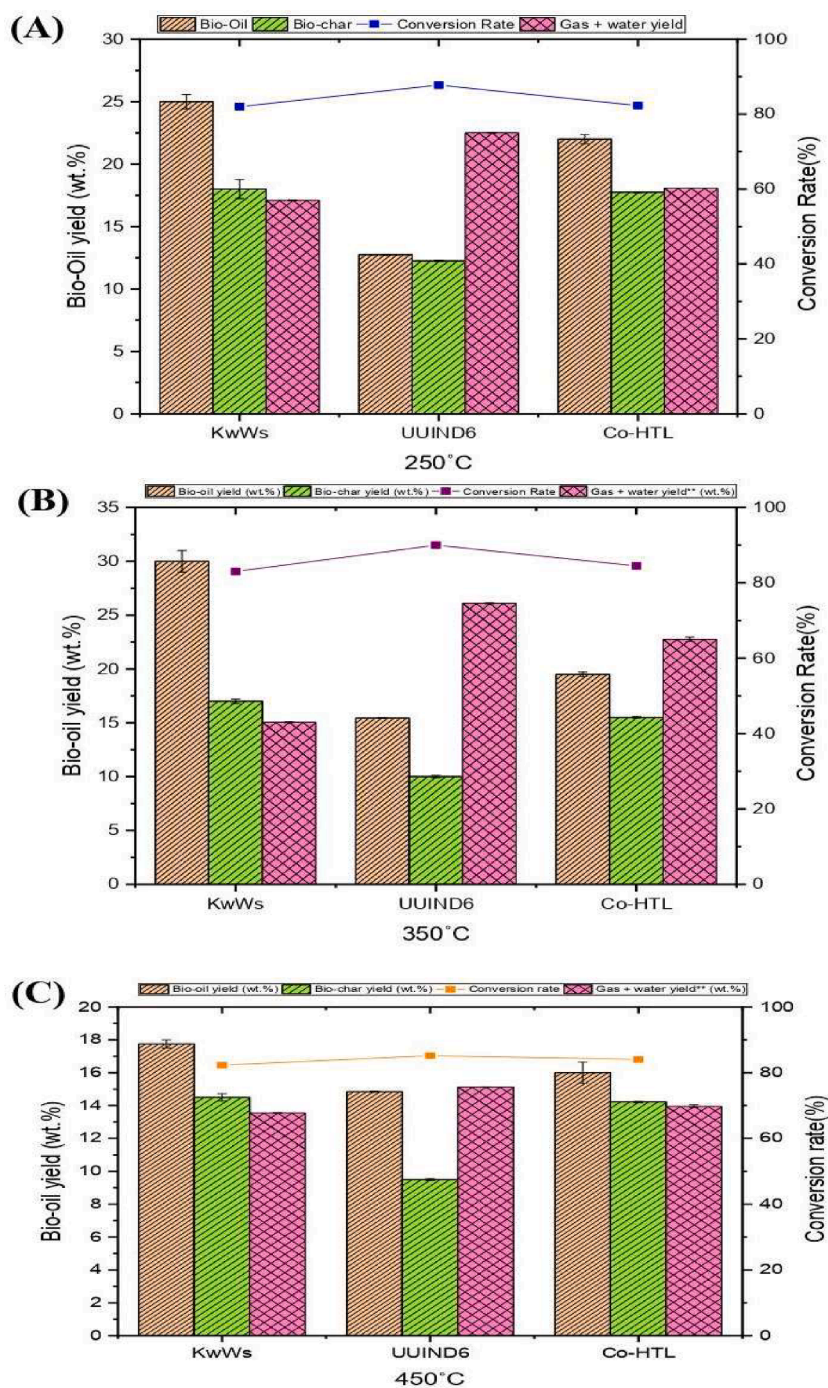


Fig. 1. Product distribution and conversion rate of KwWs, UUIND6 and Co-HTL at Multi-Stage HTL conditions.

been used as feedstock for HTL are agricultural waste, municipal waste, and algal biomass, which are the most well-known and widely used in the production of high-quality bio-oil yields, which remains the primary goal of the liquefaction process. Cellulose, hemicellulose, and lignin are the main components of lignocellulosic biomass [35], whereas algal biomass is high in carbohydrates, protein, and lipids [36].

Temperature is another important operating boundary in HTL, which has a sequential influence on the amount of liquefaction products. The main product of biomass liquefaction is bio-oil, with typical operating temperature ranging from 200 °C to 450 °C as cited in several literature. Several studies have explored liquefaction and discovered that raising reaction temperature increases bio-oil yields; nevertheless, there is a temperature limit beyond which additional temperature rise diminishes

bio-oil yields [37]. In general, the characteristics and bio-crude yields are unequivocally reliant upon increasing the reaction temperature at subcritical conditions. When the temperature exceeds the activation energy, significant bond fragmentation and depolymerisation of biomass occurs. As a result, the concentration of free radicals rises, and the repolymerizes the fragmented molecules [38]. The relationship between hydrolysis and repolymerization process are heavily influenced by the temperature.

This section of the study begins by presenting the work of three biomass (KwWs, UUIND6 and Co-HTL) with varied chemical compositions performed at different temperature conditions during Multi-Stage liquefaction process in order to investigate their effects on the bio-oil and their quality characteristics. As the bio-oil yield was more in

Table 1
Effect of different feedstock biomass and temperature condition on bio-oil yield (wt.%) at Multi-Stage HTL.

Feedstock biomass type /Temperature	Temperature (C)			Total Bio-oil Yield (wt.%)
	250C	350C	450C	
KwWs	25 ± 0.57 ^a	30 ± 1.00 ^b	17.75 ± 0.25 ^c	72.75 ± 0.37
UUIND6	12.74 ± 0.01 ^d	15.44 ± 0.04 ^f	14.85 ± 0.04 ^h	43.03 ± 0.01
Co-HTL	22 ± 0.36 ^e	19.5 ± 0.20 ^g	16 ± 0.64 ⁱ	57.5 ± 0.22

*Values are represented as mean ± standard deviations. Superscript letters with different letters in the same rows and columns indicate significant difference ($p < 0.05$) among the feedstock biomass type/temperature conditions.

Table 2
Comparative effect of various temperature and residence times during HTL of different biomasses.

Biomass type	HTL type	Optimum Temperature (C)	Residence time (min)	Maximum yield (wt.%)	References
Wood (White pine sawdust)	Single-Stage	300	15	66	[62]
Wastes (Sewage sludge)		300	40	45.51	[63]
Algae (<i>Dunaliella tertiolecta</i>)		360	50	25.8	[64]
Sludge (Paper sludge)		280	60	26	[49]
<i>Chlorella vulgaris</i>		287	40	56.21	[44]
Co-HTL (<i>Monoraphidium sp.</i> + domestic sewage sludge)		325	45	39.6	[26]
Co-HTL (Swine manure + wastewater algae)		300	60	37.5%	[65]
Kitchen wastewater sludge (KwWs)		250		25 ± 0.57	
		350	30	30 ± 1.00	
		450		17.75 ± 0.25	
		250	30	12.74 ± 0.01	Current Study
Microalgae (UUIND6)	Multi-Stage	350		15.44 ± 0.04	
		450		14.85 ± 0.04	
		250		22 ± 0.36	
Co-HTL (KwWs + UUIND6)		350	30	19.5 ± 0.20	
		450		16 ± 0.64	

Multi-Stage HTL than Single stage HTL, further Multi-Stage HTL process was used in further study to produce bio-oil and their characterization S Fig. 1 (A-C).

3.1. Effect of Multi-Stage HTL on bio-oil and bio-char yield

Fig. 1 depicts the bio-oil yields and conversion rate of different biomass samples at different temperatures in order to explore the reaction processes that occur throughout the Multi-Stage HTL process. In the present investigation, Multi-Stage HTL was only performed at the three stated temperature ranges at constant residence time on the basis of preliminary trials since low temperatures (i.e., below 250 °C) result in carbonation and high temperatures (i.e., beyond 450 °C) result in gassing since each biomass is unique and has a distinct optimal temperature for reaching the greatest and best quality bio-oil production [34,39-43]. Notably bio-oil of KwWs, which has the greatest food waste content, generates the highest bio-oil yield during the Multi-Stage HTL process (i.e., 72.75 ± 0.37 wt%), followed by Co-HTL (57.5 ± 0.22 wt%) and microalgae biomass (UUIND6) (42.03 ± 0.01 wt%) bio-oil yields from 250C to 450C as shown in Table 1. It is worth noting that an upward trend of bio-char yield was obtained at Stage-I of Multi-Stage HTL process with rising temperature and reaches the maximum for KwWs (18 ± 0.76 wt%) at 250C and decreases in Stage-II to Stage-III as temperature increases from 250C to 450C as shown in S Table 1. The solid fraction (bio-char) obtained from Stage-I was processed during Stage-II

of multi-stage HTL at 350C. The yield of the bio-oil increased and reaches maximum (30 ± 1.00 wt%) before dropping at next Stage-III at higher temperature (450C) by 17.75 ± 0.25 wt%. This maximum behaviour could be explained by the variable biomass chemical compositions and optimal temperature point for high bio-oil yields during HTL process, in other words, initial temperature increase involves increasing the efficiency. Initially, biomass rich in carbohydrates, lipids, and protein readily undergo isomerization, reforming, depolymerization, and repolymerization reactions in hot compressed water at relatively low temperatures ranges i.e., 250C to 350C at constant residence time, resulting in an upward trend thus eventually producing high bio-oil yields [44].

Once the efficiency or reaction temperatures approach a maximum or exceed the supercritical point of water, i.e., above 350C, two processes emerge to limit further liquefaction endorsing lower bio-oil yields, firstly excessive reaction temperature encourages repolymerisation and intermediate product decomposition. Secondary reactions are essentially initiated, causing intermediate products to undergo secondary reactions, hence accelerating the synthesis of boudouard gas and culminating in the generation of additional hydrocarbon gases [34,44]. Secondly, high temperatures, particularly those nearing super-critical water levels, prevent further bio-oil production because water characteristics change dramatically in super-critical conditions, reducing bio-oil yields and boosting gas formation [38,45-48]. In contrast to bio-oil yield, the solid phase yield, particularly bio-char yield, tends to rise

Table 3
Elemental analysis of different raw feedstock.

Type of Feedstock Biomass	C (%)	N (%)	H (%)	O (%)	H/C	O/C	N/C	HHV (MJ/kg)
KwWs	49.97	0.77	9.06	40.17	2.158	0.603	0.013	22.66
UUIND6	4.36	7.03	45.18	45.18	123.372	7.779	1.382	16.67
Co-HTL	40.58	3.63	7.03	48.76	2.062	0.902	0.076	15.05

Table 4
Elemental analysis of bio-oils derived from different biomasses at Multi-Stage HTL.

Temperature	Type of Feedstock Biomass	C (%)	N (%)	H (%)	O (%)	H/C	O/C	N/C	HHV (MJ/kg)	Energy Recovery (%)	Conversion Rate (%)
250C	KwWs	75.48	0.3	12.12	12.09	1.911	0.120	0.003	40.62	44.81	75
	UUIND6	59.07	4.05	8.46	28.40	1.705	0.360	0.058	26.97	20.63	87.26
	Co-HTL	69.13	0.33	11.62	18.91	2.001	0.205	0.004	36.55	53.40	78
350C	KwWs	74.94	0.7	12.18	12.16	1.935	0.121	0.008	40.52	53.64	70
	UUIND6	75.98	4.44	9.15	10.41	0.691	0.102	0.050	36.87	34.18	84.56
	Co-HTL	71.15	4.14	10.01	14.67	1.675	0.154	0.049	35.70	46.24	80.5
450C	KwWs	73.37	1.02	11.53	14.06	1.870	0.143	0.011	38.72	30.33	82.25
	UUIND6	68.84	8.01	9.01	14.13	1.558	0.154	0.099	33.59	29.97	85.15
	Co-HTL	73.2	1.46	10.66	14.66	1.724	0.150	0.017	37.32	39.66	84

due to high free-radical accumulation and initiation of repolymerization, condensation and cyclization reactions at high temperature. Both Table 1 and S Table 2 (A-F) displays the effect of different biomasses and temperature conditions on bio-oil yields. Regardless the different temperature conditions, all the treated samples showed a significant ($p < 0.05$) variation in bio-oils yield among them. Similarly, a significant ($p < 0.05$) bio-oil yields was observed along with the different temperature conditions irrespective treated samples.

The findings of bio-char and gas + water yields also validated the suggested reaction pathway of this study as shown in Fig. 1. S Table 1 and S Table 3 (P-U) displays the effect of different biomasses (treatments) and different temperature conditions on bio-char yields. Regardless of the different temperature conditions, all the treated samples showed a significant ($p < 0.05$) variation in bio-char yields among them. Similarly, a significant ($p < 0.05$) bio-char yield was observed along with the different temperature conditions irrespective of treated samples. Because of the repolymerization process, the bio-char curves for KwWs, UUIND6, and Co-HTL support the lowest solid and gaseous product yields at the same temperature of maximum bio-oil yields.

Several studies revealed that temperature and biomass composition are effective parameters of bio-crude yield quality as well as quantity, but there is always a temperature limit beyond which the biocrude yields and quality diminishes, for instance, Xu and Lancaster [49] elucidated that lowest temperature during HTL of pulp/paper sludge powder gave the maximum yield i.e., 60 wt% of total biocrude while the highest bio-crude yield (at roughly 24 wt%) was achieved at 350 °C. Furthermore, Chumbao and Etcheverry [50] discovered a plateau in the yield of biocrude oil after a certain temperature (300 °C), revealing an increase in char formation at higher temperatures due to cyclization and condensation reactions of liquid products as well as the cracking reactions of gaseous hydrocarbons.

A similar situation was reported by Sun et al. [51] investigating highest bio-crude yields in hot compressed water from Paulownia HTL obtained at 300 °C, which with subsequent increase in temperature

decreased bio-crude yields owing to competition between the two processes involved in liquefaction, hydrolysis and repolymerization. Zhong and Wei [52] validated this by studying the HTL process in *Fraxinus mandshurica*, *Cunninghamia lanceolata*, *Populus tomentosa* and *Pinus massoniana*. Guo et al. [27] investigated the temporal variations of *Cyanophyta* derived bio-crude using HTL at a temperature between 220 and 400 °C with 10% algae loading and a batch holding duration of 60 min. As shown, the highest bio-crude yield of 38.46% was recorded at 350 °C, with a declining tendency at higher temperatures down to 33.32% at 400 °C, owing to harsher reaction conditions, particularly temperatures over the critical point, which promote cleavage, steam reforming, and gasification, resulting in higher gas yields that are undesirable for bio-oil production. Similar bio-crude yield patterns at this temperature range have previously been documented for HTL of other algae strains.

Xu et al. [53] used a 10 min residence period to investigate the fluctuations of bio-crude yields and compositions of various products with temperature increase during HTL of sewage sludge ranging from 260 °C to 350 °C. Their findings demonstrated as the working temperature approached 350C, the yields began to fall. The maximum yield 22.9 wt% was observed at 340C. Durak and Genel [43] revealed that temperature is an effective parameter of bio-oil yield quantity and quality and suggested that the highest yield for light bio-oil was obtained at 280C and 300C for heavy bio-oil over a temperature range of 220-300C. This showed that polymerization processes are advantageous for the creation of light bio-oil at temperatures over 280C; however, for heavy bio-oil, both depolymerization and polymerization are effective as temperature rises.

Prior to the Multi-Stage HTL study, Single stage HTL of three biomasses (KwWs, UUIND6 and Co-HTL) were performed at three different temperatures (250C, 350C, and 450C), with each temperature corresponding to three different residence times (30 min, 60 min, and 90 min) to assimilate the effect of Single-Stage HTL on product distribution profiles, particularly bio-oil yields. The acquired findings are shown in S

Table 5
¹HNMR chemical shifts of bio-oils obtained from KwWs, UUIND6 and Co-HTL at Multi-Stage condition.

Chemical shift (ppm)	Protons	Chemical Assignment	UUIND6 bio-oil			KwWs bio-oil			Co-HTL bio-oil		
			At 250 °C	At 350 °C	At 450 °C	At 250 °C	At 350 °C	At 450 °C	At 250 °C	At 350 °C	At 450 °C
5.5–5.2	CHOCOR, CH = CH	Glyceryl and olefinic methine	–	–	–	+	–	–	+	–	–
3.7–3.5	–CO2CH3	Methyle esters	–	–	–	–	–	–	–	–	–
2.9–2.7	CH = CHCH2CH = CH	Diallylic methylenes	+	–	–	+	–	–	+	–	–
2.5–2.2	CH2COOR	Methylenes α to the carbonyl	+	–	–	+	–	–	+	–	–
2.1–1.9	CH2CH = CH	Allylic methylenes	+	–	–	+	–	–	+	–	–
1.8–1.5	CH2CH2COO–	Methylenes β to the carbonyl	+	–	–	+	–	–	+	–	–
1.4–1.0	–(CH2) _n	Other Methylenes	+	–	–	–	–	–	–	–	–
1.0–0.7	–CH ₃	Methyl	+	–	–	–	–	–	–	–	–

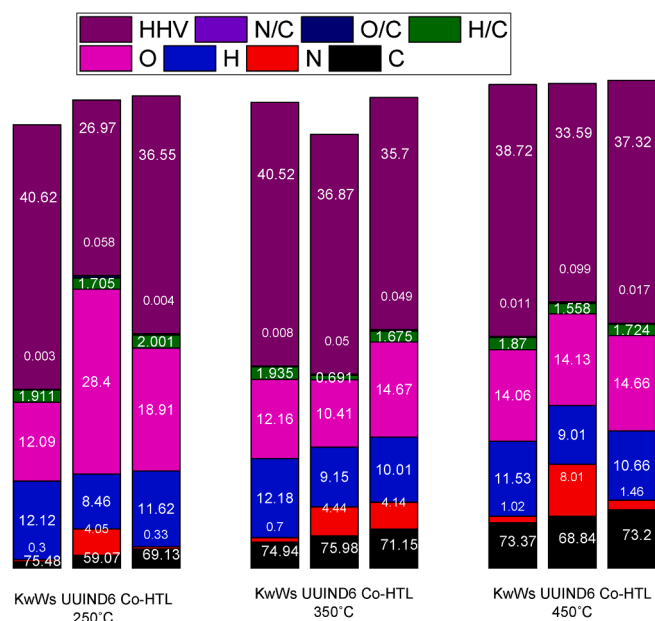


Fig. 2. Elemental composition of KwWs, UUIND6 and Co-HTL bio-oils at Multi-Stage HTL conditions.

Table 4 (A-C) and S Fig. 1 (A-C). The bio-oil yield in Single-Stage HTL was found to be highest for KwWs at 350C (34 ± 0.04 wt%) at the shortest retention or residence duration (30 min) and lowest yield for UUIND6 at 450C (7.62 ± 0.87 wt%) at the longest residence time (90 min). A similar argument was addressed above in relation to temperature. Many research, however, have investigated at the levelling-off of biocrude yields with prolonged residence time, which might be due to secondary and tertiary processes (condensation, crystallisation, re-polymerization). As a result, it was determined that increasing residence time improves biocrude yields but exceeding a certain threshold value has a negative effect, implying that the residence time threshold is dependent on certain characteristics such as biomass feed, catalyst type, and operating conditions [37]. Furthermore, the effect of this parameter is closely related to temperature LI et al. [54], for instance, Zhang et al. [55] also conducted the similar study on HTL of mixture of native grassland perennials at different residence durations ranging from 1 to 30 min, getting the maximum biocrude yields (82.1 wt%) at 1 min residence time with temperature 374 °C. As a result, multiple studies have been conducted to evaluate the effect of temperature and residence duration on various biomasses' bio-crude yields and their properties. Comparative analysis of single stage and Multi-Stage bio-oil yield was reported in Table 2.

3.2. Elemental composition of Multi-Stage derived bio-oils and bio-chars

The elemental compositions of bio-crudes obtained from three different feedstock biomass (KwWs, UUIND6, and Co-HTL) in Multi-Stage HTL under the stated experimental temperature conditions of the Multi-Stage HTL processes are shown in Table 3, 4 for bio-oils and S Table 5 for bio-chars.

It can be seen that all the three derived bio-oils were high in all the main elements i.e., carbon, nitrogen, hydrogen, and oxygen across different temperature ranges of the overall HTL process as compared to the raw feedstock biomass as shown in Fig. 2. However, there was no discernible pattern observed in the elemental compositions of all the three feedstock biomasses derived bio-oils during the Multi-Stage liquefaction process, for instance, carbon, nitrogen and oxygen content of the UUIND6 bio-oil were found to be higher than that of the KwWs and Co-HTL at 350C, 450C and 250C, respectively. This greater nitrogen and carbon concentration in UUIND6 bio-oils may be due to a

higher protein and lipid content when compared to other samples. In contrast to this, hydrogen content was observed to be higher in KwWs bio-oil at 350C followed by Co-HTL and UUIND6 derived bio-oils at 250C and 350C, respectively. Except for the O content, similar findings were seen over the same temperature ranges of the multi-stage liquefaction process in the elemental composition of the UUIND6 bio-char, which was found to be greater than that of the KwWs and Co-HTL derived bio-chars. KwWs bio-char had the highest O content (71.18%) at 450C, followed by Co-HTL (61.08%) and UUIND6 (35.32%) derived bio-chars at 450C and 250C, respectively.

• Carbon content.

Co-HTL bio-oil carbon content increased from 69.13% to 73.2% when temperature climbed from 250C to 450C, but dropped in KwWs bio-oil (75.48% to 73.37%). This, however, was not observed with UUIND6 bio-oil. A rise in temperature first resulted in an increase in carbon content in UUIND6 bio-oil ranging from 59.07% to 75.98% i.e., up to 350C, then declines at 450C to 68.84%. Similar findings have been investigated in previous studies with temperature rise results in carbon content of bio-crude, which is consistent with a larger loss of heteroatom-containing functional groups (i.e., oxygen, nitrogen, and sulphur) within the feedstock below extreme reaction conditions, which are primarily derived from proteins, lipids, carbohydrates [53,56]. Brown et al. [57] determined a comparable rise in carbon content from 74.6 wt% to 81.2 wt% with increasing temperature from 200 °C to 500 °C for isothermal HTL of *Nannochloropsis*.

With the same rising temperature ranges, the carbon content of bio-chars derived from both KwWs and Co-HTL declined from 43.84% to 24.6 % and 40.73% to 32.84%, respectively. This, however, was not the case with UUIND6 bio-chars, which showed an increase in carbon content from 48% to 59.62%. The physical and chemical characteristics of bio-char are heavily influenced by a range of factors such as processing conditions, biomass type for instance, algal bio-char demonstrates significant differences in physical and chemical properties when compared to lignocellulosic biomass [58].

• Nitrogen content.

With the same increasing temperature ranges, the nitrogen content of both KwWs and UUIND6 bio-oils rose from 0.3% to 1.02% and 4.0% to 8.01%, respectively. Co-HTL derived bio-oil exhibited an increase in nitrogen content up to 350C (0.33% to 4.14%), then declined to 1.46% at 450C. This trend of nitrogen contents increase with rising temperature is apparently explained by the fact that increasing temperature promotes initially nitrogen-containing compounds (e.g., amino acids) in the aqueous phase reacting more readily among themselves (dimerization) and also with sugars (Maillard reaction) to create hydrophobic molecules that partition into the bio-crude, thus transferring more nitrogen-containing organic compounds to form biocrude as the reaction conditions become more favourable. Denitrogenation processes, on the other hand, begin after 340C [53].

During the Multi-Stage liquefaction process, no clear trend in the nitrogen concentration of the three generated bio-chars from different feedstocks was found. Up to 350 °C, the nitrogen concentration of KwWs and Co-HTL produced bio-chars decreased from 0.36 % to 0.12 % and 1.65 % to 0.66 %, respectively, before increasing to 0.28 % and 0.29 %, respectively, at 450 °C. At the same rising temperature ranges, UUIND6 generated bio-char showed an inverse pattern, ranging from 8.88 % to 9.66 % up to 350 °C before falling to 5.40 % at 450 °C.

• Hydrogen content.

The hydrogen content of KwWs and UUIND6 generated bio-oils enhanced from 12.12% to 12.18 % and 8.46% to 9.15%, respectively, up to 350 °C before falling at 450 °C. Despite this, Co-HTL produced bio-

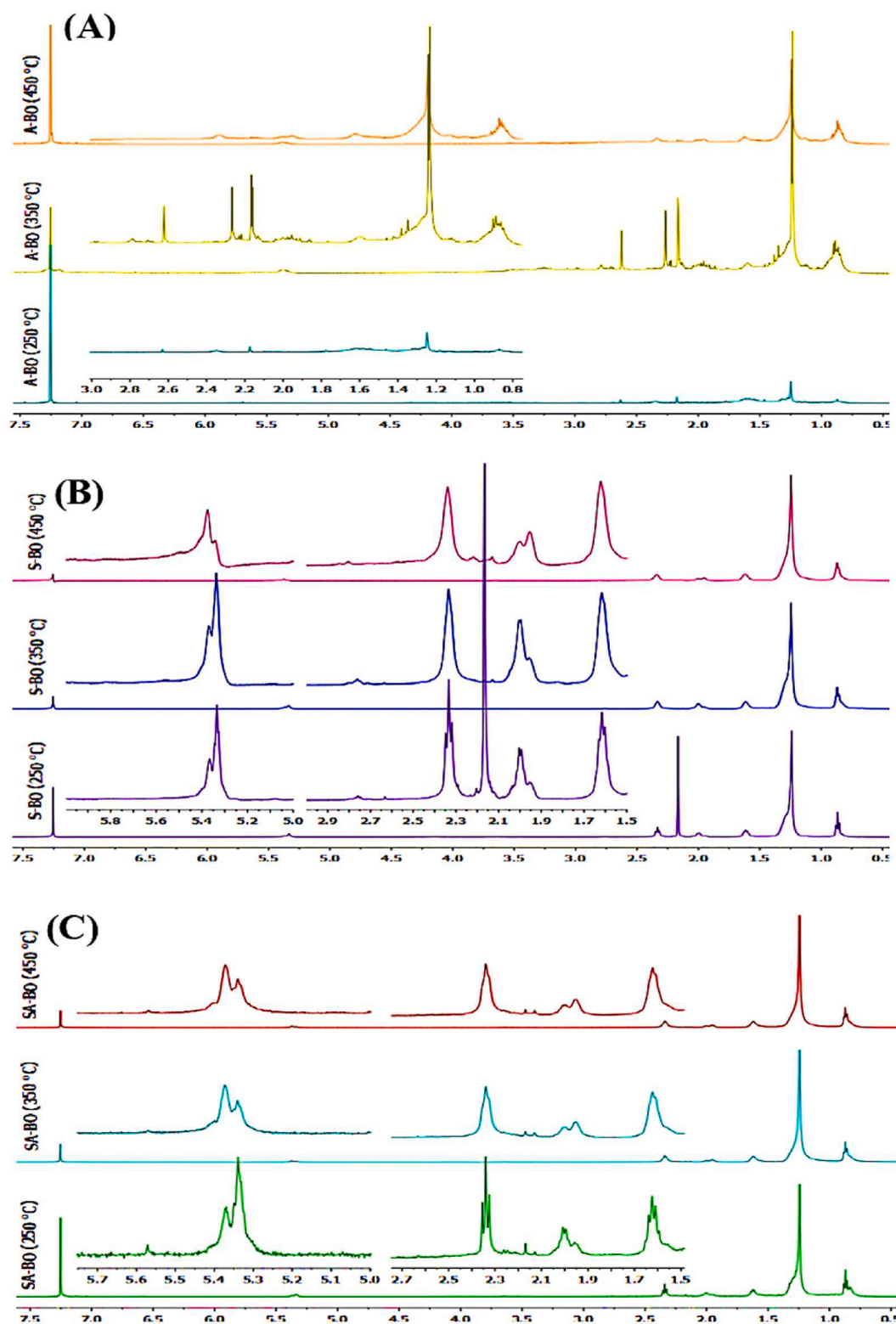


Fig. 3. ^1H NMR spectra of bio-oils from (A) UUIND6, (B) KwWs and (C) Co-HTL at Multi-Stage HTL conditions.

oil demonstrated an abrupt trend at the same temperature ranges.

Similarly, hydrogen content of KwWs and Co-HTL generated biochars dropped from 7.46 % to 3.85 % and 6.89 % to 5.77 %, respectively from 250 to 450 °C. Despite this, UUIND6 produced bio-char had a higher percentage of hydrogen content, ranging from 7.80 % to 8.34 % at the same temperature ranges.

• Oxygen content.

The oxygen content in bio-oil of KwWs. and Co-HTL showed an inverse trend at the same rising temperature ranges, ranging from 12.09% to 14.06% and 18.91% to 14.66 %, respectively. At lower temperatures (250C), UUIND6 bio-oil has a greater oxygen content (28.40%). This considerable decrease in oxygen content at high HTL temperatures

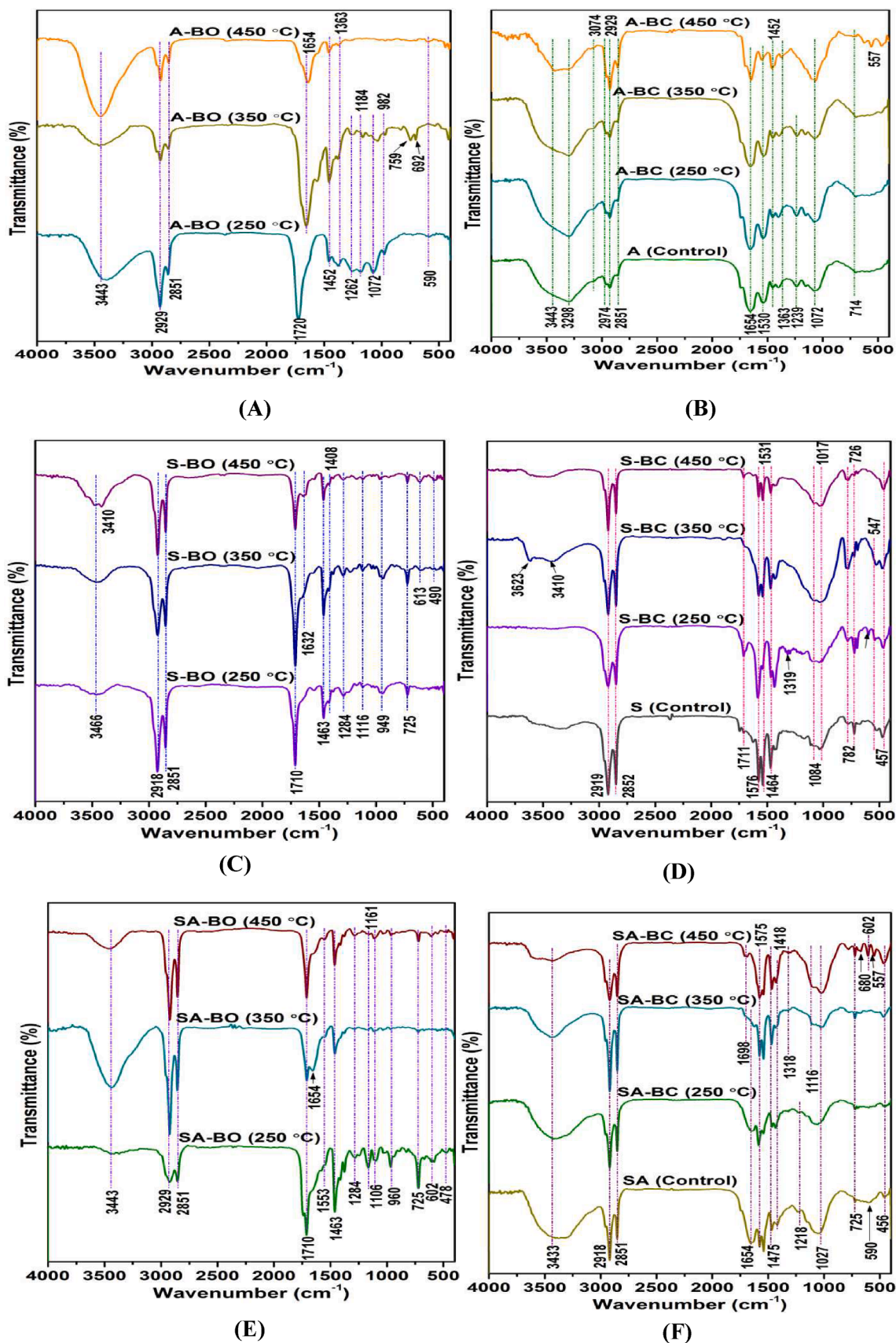


Fig. 4. FTIR Spectra of biomass (control), bio-oils and bio-chars from UUIND6 (A-B), KwWs (C-D) and Co-HTL (E-F) at Multi-Stage HTL conditions.

Table 6

FTIR band assignments for KwWs, UUIND6 and Co-HTL derived bio-oils at Multi-Stage HTL condition.

S. No.	Wavenumber (cm ⁻¹)	Bond	Functional groups/ Assignments	IR spectra of KwWs bio-oil (cm ⁻¹)			IR spectra of UUIND6 bio-oil (cm ⁻¹)			IR spectra of Co-HTL bio-oil (cm ⁻¹)		
				At 250 °C	At 350 °C	At 450 °C	At 250 °C	At 350 °C	At 450 °C	At 250 °C	At 350 °C	At 450 °C
	3500–3200 (s,b)	O-Hstretch, intermolecular H-bonded	alcohols, phenols	3466	–	3410	3443	–	–	3443	–	–
2.	3100–2850 (m)	C-Hstretch	alkenes, alkanes, aromatics	2918	–	–	2929	–	–	2929	–	–
3.	1720–1706 (s)	C=O stretch	carboxylic acid (dimer)	1710	–	–	1720	–	–	1710	–	–
4.	1710–1640 (s, m)	C=O stretch -C=C- stretch	α, β-unsaturated aldehydes and ketones, alkenes	–	1632	–	–	–	1654	–	1654	–
5.	1600–1475 (m)	C–C stretch (in-ring) N–O stretch	aromatics, nitro compound	–	–	–	–	–	–	1553	–	–
6.	1470–1450 (m)	C–H bend	alkanes	1463	–	–	1452	–	–	1463	–	–
7.	1450–1350 (m)	C–H bend C–H rock	alkanes	–	–	1408	–	–	1363	–	–	–
8.	1335–1250 (s)	C–N stretch	aromatic amines	1284	–	–	–	–	–	1284	–	–
9.	1300–1150 (m)	C–H wag (-CH ₂ X)	alkyl halides	–	–	–	1262	1184	–	–	–	1161
10.	1250–1020 (m)	C–N stretch	aliphatic amines	1116	–	–	1072	–	–	1106	–	–
11.	1000–700 (m)	C–N/ R–O–C/ R–O–CH ₃ stretching/ aromatic C–H	protein constituents	949	–	–	–	982	–	960	–	–
12.	700–500 (b,s)	C–C stretching	aliphatic groups	–	613	–	590	692	–	602	–	–

s: sharp, b: broad, m: medium.

promoted deoxygenation, most likely via decarboxylation, dehydration, and decarbonylation [44]. On the other hand, KwWs bio-char had the maximum oxygen content (71.18%) at high temperatures (450C), followed by Co-HTL generated bio-chars (61.08%). However, over the same rising temperature ranges, UUIND6 bio-char showed an inverse trend, ranging from 35.32% to 26.62%.

3.3. Characterization of bio-oils and bio-chars

3.3.1. NMR analysis

The NMR spectra of the extracted bio-oils from KwWs, UUIND6, and Co-HTL into bio-diesel were investigated using ¹H NMR spectroscopy at three different temperatures, namely 250, 350, and 450C of Multi-Stage HTL. The spectra of KwWs, UUIND6, and Co-HTL of Multi-Stage derived bio-oils are depicted in Fig. 3, and the assignments are provided in Table 5.

When the individual intensities of the respective bio-oils were compared, the presence of distinct peaks of methylenes β to the carbonyl (CH₂CH₂COO—); allylic methylenes (CH₂CH=CH); methylenes α to the carbonyl (CH₂COOR); diallyl methylenes (CH=CHCH₂CH=CH) and glyceryl and olefinic methine (CHOCOR, CH=CH) were recorded in the bio-oils extracted from KwWs and Co-HTL at 250C and were labelled at the range of 1.8–1.5 ppm; 2.1–1.9 ppm; 2.5–2.2 ppm; 2.9–2.7 ppm and 5.5–5.2, respectively. The lack of signals at 1.0–0.7 ppm, 3.7–3.5 ppm, and 1.4–1.0 ppm indicates a lack of protons implicated in the methyls (—CH₃), methylenes (—(CH₂)_n), and methyl esters (—CO₂CH₃) moiety in KwWs and Co-HTL biodiesel. UUIND6 bio-oils, on the other hand, demonstrated the existence of comparable peaks as above along with methyls (—CH₃) and methylenes (—(CH₂)_n). The production of glyceryl and olefinic methine moiety, however, was not detected in UUIND6 bio-oil.

3.3.2. FTIR analysis

The FTIR spectroscopy of all the three types of biomasses as well as their resulting bio-oils and bio-chars was explored at varied temperature conditions during multi-stage hydrothermal liquefaction by investigating the active functional groups, mode of vibration, and strength of spectra displayed in Fig. 4 and Table 6 for bio-oils and S Table 6 for bio-chars. The current study showed that FTIR analysis results of functional groups, particularly bio-oil, supplements GC–MS data.

At 250C, a sharp and broad-spectrum band between 3500 and 3200 cm⁻¹ was observed in all the three derived bio-oils, corresponding to the stretching band of intermolecular hydrogen bonding (O–H stretch), suggesting the existence of certain alcohols or phenols that may be present in the bio-oil samples. Similar functional groups were also reported in UUIND6 and Co-HTL biomass samples, indicating that UUIND6 may be responsible for the presence of these bonds in Co-HTL as well. At 3100–2850 cm⁻¹, some medium C–H and =C–H stretching sorption peaks were identified in both the generated bio-oils and bio-chars from all three biomasses, indicating the hydrolysis and degradation process of carbohydrate and lipid functional groups into hydrocarbons. The spectral bands found between 1720 and 1706 cm⁻¹ is due to C=O stretching vibrations including carboxylic acid (dimer) in KwWs biomass as well as all derived oil samples. The band regions between 1600 and 1475 cm⁻¹ indicates aromatic and nitro-compound C–C and N–O stretching in all biomass samples, Co-HTL bio-oil at 250C, and bio-chars of KwWs and Co-HTL at 450C.

The presence of alkanes owing to C–H bending in the biomass and bio-oil of KwWs, UUIND6 bio-oil and bio-char, and Co-HTL bio-oil was indicated by the band at 1470–1450 cm⁻¹.

Furthermore, the position of the strong vibration bands at 1335–1250 cm⁻¹ was ascribed to C–N functional groups, indicating the existence of aromatic amines in KwWs and Co-HTL bio-oils at 250C and bio-chars at 350C of KwWs and Co-HTL. A medium peak was observed in the band range of 1300–1150 cm⁻¹ for UUIND6 derived bio-oil at 250C

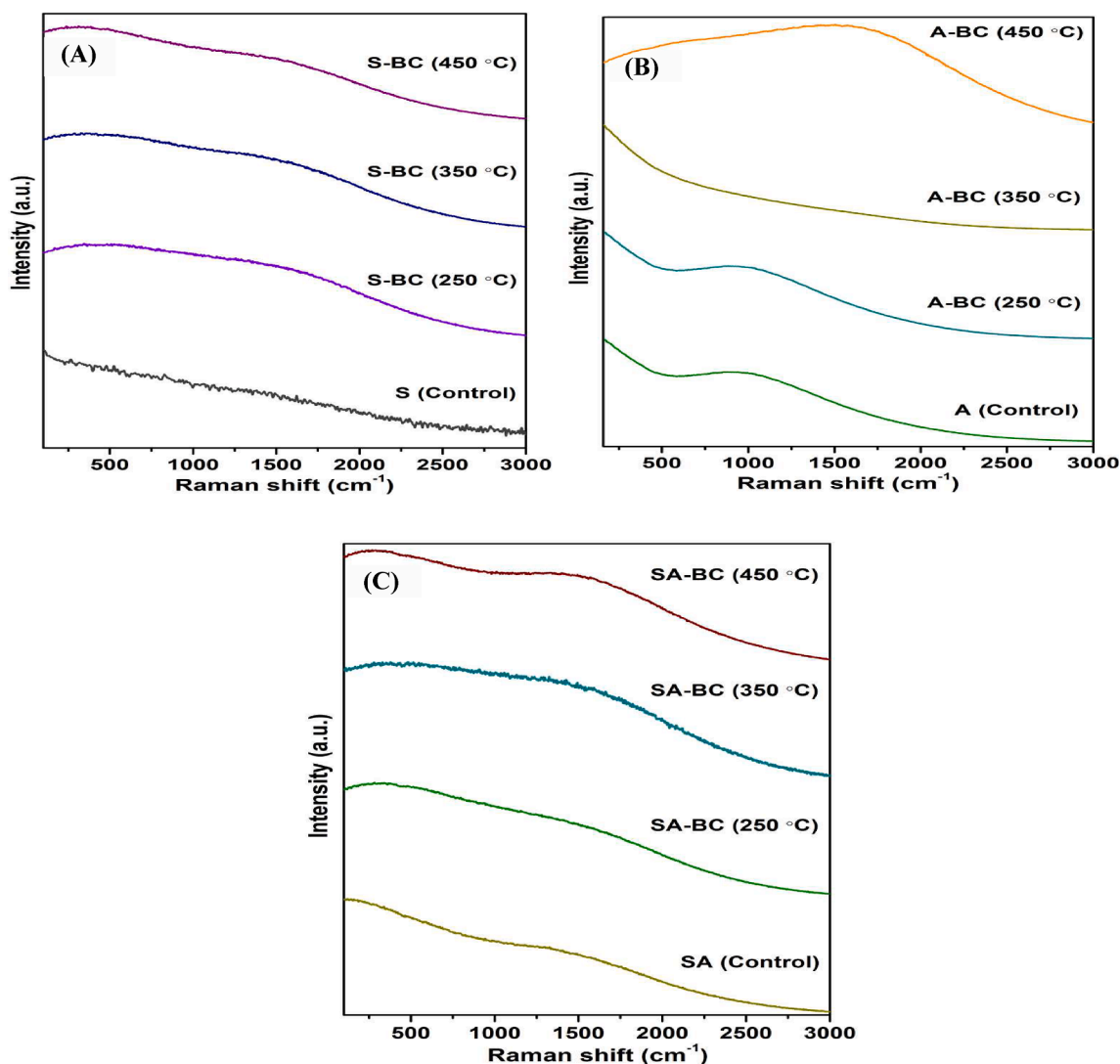


Fig. 5. Raman Spectra of biomass (control) and bio-chars from (A) KwWs, (B) UUIND6 and (C) Co-HTL at Multi-Stage HTL conditions.

as well as 350C, while for Co-HTL at 450C signified the $-\text{CH}_2\text{X}$ group for alkyl halides. Similar functional groups were discovered in UUIND6 and Co-HTL biomass samples, indicating that UUIND6 may be responsible for the presence of these bonds in Co-HTL as well. In all biomasses and bio-oil samples, the bands spanning from 1000 to 700 cm^{-1} attribute C-N/R-O-C/R-O- CH_3 stretching and aromatic C-H comprising protein components. The strong and broad peaks at 700–500 cm^{-1} confirmed the aliphatic groups owing to C-C stretching in KwWs bio-oil and bio-char samples at 350C; UUIND6 bio-oils produced at both 250C and 350C while bio-char formed at 450C; and Co-HTL biomass, bio-oil at 250C, with bio-char derived at 450C.

A strong absorbance peak of C=O and $-\text{C}=\text{C}-$ stretching at 1710–1640 cm^{-1} at 350C indicated that α , β -unsaturated aldehydes, ketones, and alkanes may exist in the three derived bio-oils and biomass of UUIND6 and Co-HTL.

At 450C, a moderately stretched band for KwWs was found at 1450–1350 cm^{-1} for C-H bending and C-H rocking groups, indicating the presence of alkanes in the oil. Also, similar findings were reported in biomass and bio-oils of UUIND6 and Co-HTL bio-chars.

3.3.3. Raman analysis

The Raman spectra show two distinct bands at 1350 cm^{-1} and 1590 cm^{-1} , which correspond to the D-band (amorphous carbon) and G-band (graphite phase), respectively [7,29]. Minor bands at 1080 cm^{-1} ,

1180 cm^{-1} , 1230 cm^{-1} , 1380 cm^{-1} , 1540 cm^{-1} , and 1680 cm^{-1} were also discovered in several other studies [59]. Previous research has revealed that fluorescence interference in the Raman spectrum of carbon-based fuels is associated with structures with abundant oxygen and hydrogens, such as C-H, O-H, C-O, which are active and quickly released from bio-chars during the liquefaction process [32,60,61].

The Raman spectroscopy of various biomass and subsequent bio-chars was investigated at various temperature conditions during multi-stage hydrothermal liquefaction by evaluating the intensity of D and G-bands at 500 cm^{-1} (Point-A) and 3000 cm^{-1} (Point-B) as shown in Fig. 5. As shown in Fig, the increase in G-band position was clearly noticed in UUIND6 derived bio-char with temperature increase from 250 to 450C compared to other KwWs and Co-HTL bio-chars. Previous researchers have discovered that an increase in the G-band position, corresponding to a drop in the D-band position in the Raman spectra of carbon materials, might primarily represent an increase in the order degree of the carbon structure [32]. It is consistent with the fact that bio-char with a lower volatile concentration has a more organized structure.

3.3.4. GC-MS analysis

Multi-Stage HTL derived bio-oil from KwWs, UUIND6 and Co-HTL was analyzed by GC-MS to identify the major constituents, which are depicted in Table. In the GC-MS analysis, all the bio-crude compounds were identified using the NIST library. The total area is not the 100%

Table 7

GC-MS results showing compounds and relative peak areas of bio-oils derived from KwWs, UIIND6 and Co-HTL at Multi-Stage condition.

Compound Name	Formula	KwWs HTL (Area %)			UIIND6 HTL (Area %)			Co-HTL (Area %)		
		At	At	At	At	At	At	At	At	At
		250 °C	350 °C	450 °C	250 °C	350 °C	450 °C	250 °C	350 °C	450 °C
1-Allyl-cyclohexane-1,2-diol	C ₉ H ₁₆ O ₂	–	1.53	2.79	3.96	1.75	1.98	–	–	2.29
2,4-Azetidinedione, 3,3-diethyl-1-methyl	C ₈ H ₁₃ NO ₂	–	–	–	1.87	1.45	–	1.81	–	–
(1S,15S)-Bicyclo[13.1.0]hexadecane-2-one	C ₁₆ H ₂₈ O	–	–	–	–	1.39	–	–	–	–
Benzenemethanol, 2-chloro-à-[[[(1-methylethyl) amino] methyl]-	C ₁₁ H ₁₆ C ₁ NO	–	–	–	–	2.53	–	–	–	–
zz2-Butenoic acid, 2-methoxy-, methyl ester	C ₆ H ₁₀ O ₃	–	–	–	4.87	1.18	–	–	–	–
Cyclooctanemethanol, à,à-dimethyl-	C ₁₁ H ₂₂ O	–	–	–	–	1.71	–	–	–	–
2,2-Diethyl-N-ethylpiperidine	C ₁₁ H ₂₃ N	–	–	–	1.87	1.45	–	1.81	–	–
3,4-Dimethyl-5-hexen-3-ol	C ₈ H ₁₆ O	–	–	2.79	–	–	–	–	–	–
2,2-Dimethyl-propyl	C ₁₀ H ₂₂ O ₃ S ₂	16.52	11.08	–	2.87	2.01	3.35	8.51	18.29	16.71
4,4-Dipropylheptane	C ₁₃ H ₂₈	–	–	–	1.96	2.83	4.75	4.55	1.96	9.55
2,3-Dehydro-4-oxo-à-ionone	C ₁₃ H ₁₆ O ₂	–	–	–	5.28	–	–	–	–	–
Dodecanoic acid	C ₁₂ H ₂₄ O ₂	1.06	–	–	–	–	–	–	–	–
Dodecane, 2,6,11-trimethyl-	C ₁₅ H ₃₂	–	–	–	–	–	1.66	–	–	–
Dodecanamide	C ₁₂ H ₂₅ NO	–	–	12.05	–	1.53	–	–	–	–
Decane, 2-methyl-	C ₁₁ H ₂₄	–	–	–	–	1.26	1.34	–	–	1.16
Decane, 3-ethyl-3-methyl-	C ₁₃ H ₂	–	–	–	1.89	1.01	1.34	–	–	1.02
Decane, 2-methyl- ester	C ₁₁ H ₂₄	–	–	–	3.11	–	3.64	–	2.57	–
Decane, 2,4,6-trimethyl-	C ₁₃ H ₂₈	–	–	–	2.66	2.17	2.92	–	2.25	–
2,4-Di-tert-butylphenol	C ₁₄ H ₂₂ O	–	–	–	3.33	1.32	5.20	–	1.93	1.15
7,7-Diethylheptadecane	C ₂₁ H ₄₄	–	–	–	–	–	1.22	–	–	–
Eicosane	C ₂₀ H ₄₂	–	–	–	4.08	–	–	–	–	–
Eicosane, 2-methyl-	C ₂₁ H ₄₄	–	–	–	4.5	2.24	3.12	2.55	1.86	1.7
9-Eicosenoic acid, (Z)-	C ₂₀ H ₃₈ O ₂	–	–	–	–	2.71	–	–	–	–
2-Ethyl-1-dodecanol	C ₁₄ H ₃₀ O	–	–	–	–	1.12	–	–	–	–
2-Ethylamino-1-phenylpropanol	C ₁₁ H ₁₇ NO	–	2.74	–	–	–	–	–	–	–
3-Ethyl-7-hydroxyphthalide	C ₁₀ H ₁₀ O ₃	–	–	–	–	1.74	2.24	–	–	–
2-Fluoro-6-trifluoromethylbenzoic acid, 2,3,4,6-tetra-chlorophenyl ester	C ₁₄ H ₄ C ₁₄ F ₄ O ₂	–	–	–	–	–	1.20	–	–	11.15
4-Fluoro-2-trifluoromethylbenzoic acid, 2,4,5-trichloro-phenyl ester	C ₁₄ H ₅ C ₁₃ F ₄ O ₂	–	–	–	–	1.32	–	–	–	–
5-Fluoro-2-trifluoromethylbenzoic acid, 2-formyl-4,6-dichlorophenyl ester	C ₁₅ H ₆ C ₁₂ F ₄ O ₃	–	–	–	1.33	–	–	–	1.93	–
6-Fluoro-2-trifluoromethylbenzoic acid, 2-formyl-4,6-dichlorophenyl ester	C ₁₅ H ₆ C ₁₂ F ₄ O ₃	–	–	–	3.33	1.32	1.20	–	7.93	1.15
Hexadecanamide	C ₁₆ H ₃₃ NO	–	–	12.05	–	–	–	–	–	–
Heneicosane	C ₂₁ H ₄₄	–	–	–	8.08	–	–	–	–	–
2-Hexyl-1-octanol	C ₁₄ H ₃₀ O	46.52	37.20	7.56	1.54	2.75	1.62	2.79	2.94	11.65
Heptane, 3,3-dimethyl-ester	C ₉ H ₂₀	–	–	–	1.52	3.63	5.3	–	–	–
2,4-Heptanedione	C ₇ H ₁₂ O ₂	–	–	–	1.61	1.53	–	–	–	–
2-Heptadecenal	C ₁₇ H ₃₂ O	–	–	1.06	–	–	–	–	–	1.61
3-Heptadecenal	C ₁₇ H ₃₂ O	–	–	–	–	–	3.60	–	–	–
Hexane, 3,3-dimethyl-ester	C ₈ H ₁₈	–	–	–	1.53	2.26	5.94	–	3.98	–
1-Hexyl-1-nitrocyclohexane	C ₁₂ H ₂₃ NO ₂	–	–	–	3.96	–	–	4.91	–	–
1-Hexyl-2-nitrocyclohexane	C ₁₂ H ₂₃ NO ₂	17.75	18.83	2.40	2.69	1.52	–	3.91	6.36	–
1-Hydroxycyclohexanecarboxylic acid	C ₇ H ₁₂ O ₃	–	–	–	–	–	1.14	–	–	–
1-Hexadecen-3-ol	C ₂₀ H ₄₀ O	–	–	–	–	2.58	–	–	–	–
2,2,3,3,4,4-Hexamethyltetrahydrofu- ran	C ₁₀ H ₂₀ O	–	–	–	2.27	–	–	–	–	–
1,1,1,3,5,5,5-Heptamethyltrisiloxane	C ₇ H ₂₂ O ₂ Si ₃	–	–	–	1.33	–	–	–	–	–
1,1,1,5,7,7-Heptamethyl-3,3-bis(trimethylsiloxy) tetrasiloxane	C ₁₃ H ₄₀ O ₅ Si ₆	–	–	–	–	1.97	–	–	–	–
Hexadecanoic acid, 2-hydroxy-1-(hydroxymethyl)ethyl ester	C ₁₉ H ₃₈ O ₄	–	–	–	–	–	3.60	–	–	–
5-Iodo-nonane	C ₉ H ₁₉ I	–	–	–	2.61	–	–	–	3.01	–
1-Iodo-2-methylundecane	C ₃₀ H ₆₂	–	–	–	4.18	4.11	2.45	–	–	–
Isopropyl myristate	C ₁₇ H ₃₄ O ₂	–	–	1.14	–	3.40	2.73	–	3.18	1.95
2-Isopropyl-5-methylcyclohexyl	C ₃₀ H ₃₃ ClO ₆	–	–	–	3.96	1.35	–	–	–	–
10-Methylnonadecane	C ₂₀ H ₄₂	–	–	–	1.38	2.16	–	–	–	–
2-Methyl-6-methylene-octa-1,7-dien-3-ol	C ₁₀ H ₁₆ O	–	–	–	–	1.12	–	–	–	–
3-Methyl-2-(2-oxopropyl) furan	C ₈ H ₁₀ O ₂	–	12.19	8.38	2.88	2.49	8.5	3.17	11.32	11.64
5-Methyl-2-ethenyl-cyclohexane-1- carboxylic acid	C ₁₀ H ₁₆ O ₂	–	–	–	–	1.25	–	–	–	–
5,8-Methano-1,7-dioxacyclopent[cd] azulene-2,6-dione, octahydro-2a,9-dihydroxy-8b-methy 1-9-(1- methylethyl)-	C ₁₅ H ₂₀ O ₆	–	–	–	–	–	–	6.8	5.07	–
3-Nonanone, 2-methyl-	C ₁₀ H ₂₀ O	–	–	–	–	1.19	–	–	–	–
Nonadecane, 2-methyl-	C ₂₀ H ₄₂	–	–	–	1.52	1.09	1.29	–	1.77	1.58
1-Octanol, 2-butyl-	C ₁₂ H ₂₆ O	–	–	17.56	–	–	–	1.63	–	–
Octadecane, 2-methyl-	C ₁₉ H ₄₀	–	–	–	2.34	2.94	7.96	–	13.65	1.08
9-Octadecenoic acid	C ₁₈ H ₃₄ O ₂	8.75	4.83	8.46	–	–	–	4.91	–	4.61
Pentadecanoic acid	C ₁₅ H ₃₀ O ₂	–	–	3.69	–	–	–	–	–	–
Pentanoic acid, 1,1-dimethylpropyl ester	C ₁₀ H ₂₀ O ₂	–	–	–	1.52	1.05	2.32	–	–	–

(continued on next page)

Table 7 (continued)

Compound Name	Formula	KwWs HTL (Area %)			UUIND6 HTL (Area %)			Co-HTL (Area %)		
		At	At	At	At	At	At	At	At	At
		250 °C	350 °C	450 °C	250 °C	350 °C	450 °C	250 °C	350 °C	450 °C
10-Pentadecen-5-yn-1-ol	C ₁₅ H ₂₆ O	–	–	–	–	1.55	–	–	–	–
Pentane, 2,2,3,3-tetramethyl-	C ₉ H ₂₀	–	–	–	1.01	–	–	–	1.41	–
2-Pentadecanone, 6,10,14-trimethyl-	C ₁₈ H ₃₆ O	–	–	–	–	–	1.55	–	–	–
4-Piperidinone, 2,2,6,6-tetramethyl-	C ₉ H ₁₇ NO	–	–	–	1.87	1.45	–	1.81	–	–
i-Propyl 12-methyl-tridecanoate	C ₁₇ H ₃₄ O ₂	–	–	1.14	–	3.40	4.73	–	12.18	1.95
5,10-Pentadecadien-1-ol, (E,E) (Z,Z)-	C ₁₅ H ₂₈ O	–	–	–	–	1.62	–	–	–	–
5,10-Pentadecadienoic acid	C ₁₅ H ₂₆ O ₂	–	–	–	–	1.1	–	–	–	–
6-Tetradecanesulfonic acid, butyl ester	C ₁₈ H ₃₈ O ₃ S	–	–	–	1.21	3.93	2.14	3.95	–	2.47
Tetradecane, 1-iodo-	C ₁₄ H ₂₉ I	–	–	–	1.05	3.94	1.59	–	–	–
Tetradecanoic acid	C ₁₄ H ₂₈ O ₂	5.30	4.08	3.48	–	–	–	–	–	1.78
Tridecanoic acid	C ₁₃ H ₂₆ O ₂	2.30	–	–	–	–	–	–	–	–
Tetradecanamide	C ₁₄ H ₂₉ NO	–	–	3.05	–	2.53	–	–	–	–
Tridecanol, 2-ethyl-2-methyl-	C ₁₆ H ₃₄ O	–	–	–	1.06	–	2.07	–	–	–
2,4,4-Trimethyl-3-hydroxymethyl-5 a-(3-methyl-but-2-enyl)-cyclohexene	C ₁₅ H ₂₆ O	–	–	–	1.60	–	–	–	–	–
2,6,10,14-Tetramethylpentadecan-2-ol	C ₁₉ H ₄₀ O	–	–	1.17	–	2.71	–	1.12, 1.26	–	–
2,6,10,14-Tetramethylpentadecan-3-one	C ₁₉ H ₃₈ O	–	–	–	–	2.0	–	–	–	–
2,6,10,14-Tetramethylpentadecan-5-one	C ₁₉ H ₃₈ O	–	–	–	–	1.53	–	–	–	–
2,6,10,14-Tetramethylpentadecan-6-ol	C ₁₉ H ₄₀ O	1.62	7.20	4.69	–	1.12	2.72	–	6.91	–
Tetradecane, 2,6,10-trimethyl-	C ₁₇ H ₃₆	–	–	–	–	–	1.14	–	–	–
1,2,4-Thiadiazol-5-amine, 3-(phenylmethyl)-	C ₉ H ₉ N ₃ S	–	–	–	–	–	–	1.64	–	–
Undecane, 2-methyl-	C ₁₂ H ₂₆	–	–	–	–	–	1.64	–	–	–
1,2,3-Trimethyl-5-(2-thia-n-hexyl)piperid-4-one	C ₁₃ H ₂₅ NOS	–	–	–	–	1.19	–	–	–	–

since there are unidentified peaks and furthermore the compounds were recognized based on retention area % >1. Overall, GC–MS results revealed that high temperatures encourage more diversified composition, and even more compounds were identified, including ketones, amides, cyclic dipeptides and ethers, and alkanes. In all bio-oil samples of varying biomasses at Multi-Stage HTL conditions as shown in Table 7. According to the current study, 97 chemical compounds emerged from this Multi-Stage liquefaction process, with the most prominent chemical compounds derived from bio-oil samples being in the C₆ to C₃₀ range, which were further classified into groups of aliphatic (alkanes and their derivatives), (aldehydes, esters, ketones, and carboxylic acids), monoaromatic (benzene and its), nitrogenous compounds (amines, and amides such as pyridine, pyrimidine, and pyrazole) and poly-aromatic compounds (naphthalene and indine) and oxygenated compounds (aldehydes, esters, ketones).

The major liquefaction compounds identified in the GC–MS analysis of bio-oil extracted from KwWs between temperature range 250–450°C were 2,2-Dimethylpropyl; 2-Hexyl-1-Octanol; 1-Hexyl-2-nitrocyclohexane; 3-Methyl-2-(2-oxopropyl furan); 9-Octadecenoic acid and 2,6,10,14-Tetramethylpentadecane-6-ol. On the other hand, bio-oils derived from UUIND6 and Co-HTL process showed almost similar compounds except 4,4-Dipropyl heptane; Eicosane-2-methyl; Nonadecane-2-methyl and Octadecane-2-methyl.

4. Conclusion

The production of bio-oil using Multi-Stage HTL of KwWs, UUIND6, and Co-HTL was explored at constant residence duration of 30 min. Each of the aforementioned feedstocks comprises varying organic and inorganic fractions, resulting in varying compositions of bio-oils and bio-char. Prior to the Multi-Stage HTL study, Single-Stage HTL of three biomasses was performed at the same temperature ranges temperature but corresponding to three different residence times (30 min, 60 min, and 90 min) The highest bio-oil yield was found for KwWs at 350°C (34 ± 0.04 wt%) at shortest residence duration (30 min).

According to the current study findings of Multi-Stage HTL process, the maximum bio-oil production was obtained from KwWs (i.e., 72.75 ± 0.37 wt%), followed by Co-HTL (57.5 ± 0.22 wt%) and UUIND6 (42.03 ± 0.01 wt%) bio-oil yields from 250°C to 450°C with a residence time of 30 min. The KwW sludge was rich in residues of bread, rice and

vegetables etc. Thus, the current study validates that KwWs appears to be the most suitable in terms of efficiency and renewability, with HHV of 40.52 MJ/kg and Energy Recovery of 53.64 wt%, which is greater than the UUIND6 and Co-HTL, and can thus simultaneously mitigate and convert sludge into energy-dense bio-oil under a sustainable biorefinery approach at optimal time–temperature combination for increased bio-oil yields. The presented Multi-Stage HTL process was found to be advantageous because it could achieve higher conversions and bio-oil yields compared to Single-Stage HTL by recovering and reusing the same solid fraction (bio-char) obtained from Stage-I throughout Stage-II and Stage-III while decreasing gas and heavy product outputs. As a result, this research was used to provide the groundwork for the design and implementation of laboratory-scale technological systems for bio-fuel production.

CRediT authorship contribution statement

Bhawna Bisht: Conceptualization, Methodology, Writing – original draft. **Prateek Gururani:** Formal analysis, Investigation, Data curation. **Shivam Pandey:** . **Krishna Kumar Jaiswal:** Formal analysis. **Sanjay Kumar:** Methodology, Data curation. **Mikhail S. Vlaskin:** Formal analysis, Writing – review & editing. **Monu Verma:** Formal analysis, Writing – review & editing. **Hyunook Kim:** Writing – review & editing. **Vinod Kumar:** Conceptualization, Supervision, Methodology.

Declaration of Competing Interest

The authors declare that they have no known competing financial interests or personal relationships that could have appeared to influence the work reported in this paper.

Data availability

No data was used for the research described in the article.

Acknowledgements

This paper has been supported by the RUDN University Strategic Academic Leadership Program. Monu Verma would like to thank to the National Research Foundation of Korea (NRF) for providing funding for

Brain Pool Fellowship Program (2019H1D3A1A01102657). H. Kim was supported by the Korea Environment Industry & Technology Institute (KEITI) through the project for “Development of demonstration technology for energy conversion using unused complex biomass (NO.2022003480001)” and Post-plastic Graduate Program funded by Korea Ministry of Environment (MOE).

Appendix A. Supplementary data

Supplementary data to this article can be found online at <https://doi.org/10.1016/j.fuel.2022.125253>.

References

- Atashgahi S, Aydin R, Dimitrov MR, Sipkema D, Hamonts K, Lahti L, et al. Impact of a wastewater treatment plant on microbial community composition and function in a hyporheic zone of a eutrophic river. *Sci Rep* 2015;5(1):1–3.
- Shchegolkova NM, Krasnov GS, Belova AA, Dmitriev AA, Kharitonov SL, Klimina KM, et al. Microbial community structure of activated sludge in treatment plants with different wastewater compositions. *Front Microbiol* 2016;7:90.
- Kumar V, Jaiswal KK, Vlaskin MS, Nanda M, Tripathi MK, Gururani P, et al. Hydrothermal liquefaction of municipal wastewater sludge and nutrient recovery from the aqueous phase. *Biofuels* 2020;1–6.
- Ghenai C, Albawab M, Bettayeb M. Sustainability indicators for renewable energy systems using multi-criteria decision-making model and extended SWARA/ARAS hybrid method. *Renew Energy* 2020;146:580–97.
- Kim Y, Parker W. A technical and economic evaluation of the pyrolysis of sewage sludge for the production of bio-oil. *Bioresour Technol* 2008;99(5):1409–16.
- Huang HJ, Yuan XZ, Li BT, Xiao YD, Zeng GM. Thermochemical liquefaction characteristics of sewage sludge in different organic solvents. *J Anal Appl Pyrolysis* 2014;109:176–84.
- Stancin H, Mikulčić H, Wang X, Duić N. A review on alternative fuels in future energy system. *Renew Sust Energ Rev* 2020;128:109927.
- Mayer FD, Brondani M, Carrillo MC, Hoffmann R, Lora EE. Revisiting energy efficiency, renewability, and sustainability indicators in biofuels life cycle: Analysis and standardization proposal. *J Clean Prod* 2020;252:119850.
- de Caprariis B, De Filippis P, Petruillo A, Scarsella M. Hydrothermal liquefaction of biomass: Influence of temperature and biomass composition on the bio-oil production. *Fuel* 2017;208:618–25.
- Kabir G, Hameed BH. Recent progress on catalytic pyrolysis of lignocellulosic biomass to high-grade bio-oil and bio-chemicals. *Renew Sust Energ Rev* 2017;70:945–67.
- Ellersdorfer M. Hydrothermal co-liquefaction of *Chlorella vulgaris* with food processing residues, green waste and sewage sludge. *Biomass Bioenergy* 2020;142:105796.
- Seiple TE, Coleman AM, Skaggs RL. Municipal wastewater sludge as a sustainable bioresource in the United States. *J Environ Manage* 2017;197:673–80.
- Fonts I, Gea G, Azuara M, Ábrejo J, Arauzo J. Sewage sludge pyrolysis for liquid production: a review. *Renew Sust Energ Rev* 2012;16(5):2781–805.
- Pham M, Schideman L, Scott J, Rajagopalan N, Plewa MJ. Chemical and biological characterization of wastewater generated from hydrothermal liquefaction of *Spirulina*. *Environ Sci Technol* 2013;47(4):2131–8.
- Durak H. Hydrothermal liquefaction of *Glycyrrhiza glabra* L. (Licorice): Effects of catalyst on variety compounds and chromatographic characterization. *Energy Sources Part A* 2020;42(20):2471–84.
- Gururani P, Bhatnagar P, Bisht B, Jaiswal KK, Kumar V, Kumar S, et al. Recent advances and viability in sustainable thermochemical conversion of sludge to bio-fuel production. *Fuel* 2022;2022(316):123351.
- Vardon DR, Sharma BK, Scott J, Yu G, Wang Z, Schideman L, et al. Chemical properties of biocrude oil from the hydrothermal liquefaction of *Spirulina* algae, swine manure, and digested anaerobic sludge. *Bioresour Technol* 2011;02(17):8295–303.
- Elliott DC, Biller P, Ross AB, Schmidt AJ, Jones SB. Hydrothermal liquefaction of biomass: Developments from batch to continuous process. *Bioresour Technol* 2015;178:147–56.
- WERE. Energy Production and Efficiency Fact Sheet. http://www.were.org/c/KnowledgeAreas/Energy/Latest_News/2016/Energy_Production_and_Efficiency_Fact_Sheet_2016.aspx. 2016. Accessed on 6 April, 2022.
- Rizzardini CB, Goi D. Sustainability of domestic sewage sludge disposal. *Sustainability* 2016;6(5):2424–34.
- Mishra S, Roy M, Mohanty K. Microalgal bioenergy production under zero-waste biorefinery approach: recent advances and future perspectives. *Bioresour Technol* 2019;292:122008.
- Brilman DW, Drabik N, Wądrzyk M. Hydrothermal co-liquefaction of microalgae, wood, and sugar beet pulp. *Biomass Convers Biorefin* 2017;7(4):445–54.
- Feng H, Zhang B, He Z, Wang S, Salih O, Wang Q. Study on co-liquefaction of *Spirulina* and *Spartina alterniflora* in ethanol-water co-solvent for bio-oil. *Energy* 2018;155:1093–101.
- Hu Y, Feng S, Bassi A, Xu CC. Improvement in bio-crude yield and quality through co-liquefaction of algal biomass and sawdust in ethanol-water mixed solvent and recycling of the aqueous by-product as a reaction medium. *Energy Convers Manag* 2018;171:618–25.
- Chen X, Peng X, Ma X, Wang J. Investigation of Mannich reaction during co-liquefaction of microalgae and sweet potato waste. *Bioresour Technol* 2019;284:286–92.
- Mishra S, Mohanty K. Co-HTL of domestic sewage sludge and wastewater treatment derived microalgal biomass—An integrated biorefinery approach for sustainable biocrude production. *Energy Convers Manag* 2020;204:112312.
- Guo Y, Song W, Lu J, Ma Q, Xu D, Wang S. Hydrothermal liquefaction of Cyanophyta: Evaluation of potential bio-crude oil production and component analysis. *Algal Res* 2015;11:242–7.
- Kumar V, Kumar A, Nanda M. Pretreated animal and human waste as a substantial nutrient source for cultivation of microalgae for biodiesel production. *Environ Sci Pollut Res* 2018;25(22):22052–9.
- Arora N, Philippidis GP. Insights into the physiology of *Chlorella vulgaris* cultivated in sweet sorghum bagasse hydrolysate for sustainable algal biomass and lipid production. *Sci Rep* 2021;11(1):1–4.
- Bisht B, Kumar V, Gururani P, Tomar MS, Nanda M, Vlaskin MS, et al. The potential of nuclear magnetic resonance (NMR) in metabolomics and lipidomics of microalgae—a review. *Arch Biochem Biophys* 2021;710:108987.
- Arora N, Patel A, Pruthi PA, Pruthi V. Synergistic dynamics of nitrogen and phosphorous influences lipid productivity in *Chlorella minutissima* for biodiesel production. *Bioresour Technol* 2016;213:79–87.
- Xu J, Liu J, Ling P, Zhang X, Xu K, He L, et al. Raman spectroscopy of bio-char from the pyrolysis of three typical Chinese biomasses: A novel method for rapidly evaluating the bio-char property. *Energy* 2020;202:117644.
- Islam MB, Khalekuzzaman M, Kabir SB, Hossain MR. Shrimp waste-derived chitosan harvested microalgae for the production of high-quality biocrude through hydrothermal liquefaction. *Fuel* 2022;320:123906.
- Xue Y, Chen H, Zhao W, Yang C, Ma P, Han S. A review on the operating conditions of producing bio-oil from hydrothermal liquefaction of biomass. *Int J Energy Res* 2016;40(7):865–77.
- Wu Z, Zhang J, Zhang B, Guo W, Yang G, Yang B. Synergistic effects from co-pyrolysis of lignocellulosic biomass main component with low-rank coal: Online and offline analysis on products distribution and kinetic characteristics. *Appl Energy* 2020;276:115461.
- Ali J, Wang L, Waseem H, Song B, Djellabi R, Pan G. Turning harmful algal biomass to electricity by microbial fuel cell: A sustainable approach for waste management. *Environ Pollut* 2020;266:115373.
- Dimitriadis A, Bezegegianni S. Hydrothermal liquefaction of various biomass and waste feedstocks for biocrude production: A state of the art review. *Renew Sust Energ Rev* 2017;68:113–25.
- Akhtar J, Amin NA. A review on process conditions for optimum bio-oil yield in hydrothermal liquefaction of biomass. *Renew Sust Energ Rev* 2011;15(3):1615–24.
- Qu Y, Wei X, Zhong C. Experimental study on the direct liquefaction of 107 *Cunninghamia lanceolata* in water. *Energy* 2003;28(7):597–606.
- Yin S, Dolan R, Harris M, Tan Z. Subcritical hydrothermal liquefaction of cattle manure to bio-oil: Effects of conversion parameters on bio-oil yield and characterization of bio-oil. *Bioresour Technol* 2010;101(10):3657–64.
- Jena U, Das KC, Kastner JR. Effect of operating conditions of thermochemical liquefaction on biocrude production from *Spirulina platensis*. *Bioresour Technol* 2011;102(10):6221–9.
- Anastasakis K, Ross AB. Hydrothermal liquefaction of the brown macro-alga *Laminaria Saccharina*: Effect of reaction conditions on product distribution and composition. *Bioresour Technol* 2011;102(7):4876–83.
- Durak H, Genel S. Catalytic hydrothermal liquefaction of *Lactuca scariola* with a heterogeneous catalyst: The investigation of temperature, reaction time and synergistic effect of catalysts. *Bioresour Technol* 2020;309:123375.
- Moazezi MR, Bayat H, Tavakoli O, Hallajisani A. Hydrothermal liquefaction of *Chlorella vulgaris* and catalytic upgrading of product: Effect of process parameter on bio-oil yield and thermodynamics modeling. *Fuel* 2022;318:123595.
- Chen J. Bio-oil production from hydrothermal liquefaction of *Pteris vittata* L.: Effects of operating temperatures and energy recovery. *Bioresour Technol* 2018;265:320–7.
- Yang JH, Shin HY, Ryu YJ, Lee CG. Hydrothermal liquefaction of *Chlorella vulgaris*: Effect of reaction temperature and time on energy recovery and nutrient recovery. *J Ind Eng Chem* 2018;68:267–73.
- Chen M, Li Y, Li P, Wang W, Qi L, Li P, et al. A novel native bioenergy green alga can stably grow on waste molasses under variable temperature conditions. *Energy Convers Manag* 2019;196:751–8.
- Biswas B, Kumar AA, Bisht Y, Singh R, Kumar J, Bhaskar T. Effects of temperature and solvent on hydrothermal liquefaction of *Sargassum tenerrimum* algae. *Bioresour Technol* 2017;242:344–50.
- Xu C, Lancaster J. Conversion of secondary pulp/paper sludge powder to liquid oil products for energy recovery by direct liquefaction in hot-compressed water. *Water Res* 2008;42(6–7):1571–82.
- Xu C, Etcheverry T. Hydro-liquefaction of woody biomass in sub- and super-critical ethanol with iron-based catalysts. *Fuel* 2008;87(3):335–45.
- Sun P, Heng M, Sun S, Chen J. Direct liquefaction of paulownia in hot compressed water: Influence of catalysts. *Energy* 2010;35(12):5421–9.
- Zhong C, Wei X. A comparative experimental study on the liquefaction of wood. *Energy* 2004;29(11):1731–41.
- Xu D, Lin G, Liu L, Wang Y, Jing Z, Wang S. Comprehensive evaluation on product characteristics of fast hydrothermal liquefaction of sewage sludge at different temperatures. *Energy* 2018;159:686–95.
- Li RD, Li BS, Yang TH, Xie YH. Liquefaction of rice stalk in sub- and supercritical ethanol. *J Fuel Chem Technol* 2013;41(12):1459–65.

- [55] Zhang B, von Keitz M, Valentas K. Thermochemical liquefaction of high-diversity grassland perennials. *J Anal Appl Pyrolysis* 2009;84(1):18–24.
- [56] Motavaf B, Savage PE. Effect of process variables on food waste valorization via hydrothermal liquefaction. *ACS ES&T Engineering* 2021;1(3):363–74.
- [57] Brown TM, Duan P, Savage PE. Hydrothermal liquefaction and gasification of *Nannochloropsis* sp. *Energy Fuels* 2010;24(6):3639–46.
- [58] Bhatnagar P, Gururani P, Bisht B, Kumar V. Algal Bio-char: An Advance and Sustainable Method for Wastewater Treatment. *Octa. J Biosci* 2021;9(2).
- [59] Wang H, Wang H, Zhao H, Yan Q. Adsorption and Fenton-like removal of chelated nickel from Zn-Ni alloy electroplating wastewater using activated bio-char composite derived from Taihu blue algae. *Chem Eng J* 2020;379:122372.
- [60] Xiang J, Liu J, Xu J, Su S, Tang H, Hu Y, et al. The fluorescence interference in Raman spectrum of raw coals and its application for evaluating coal property and combustion characteristics. *Proc Combust Inst* 2019;37(3):3053–60.
- [61] Xu J, Liu J, Zhang X, Ling P, Xu K, He L, et al. Chemical imaging of coal in micro-scale with Raman mapping technology. *Fuel* 2020;264:116826.
- [62] Cheng S, D'cruz I, Wang M, Leitch M, Xu C. Highly efficient liquefaction of woody biomass in hot-compressed alcohol– water co-solvents. *Energy Fuels* 2010;24(9):4659–67.
- [63] Malins K, Kampars V, Brinks J, Neibolte I, Murnieks R, Kampare R. Bio-oil from thermo-chemical hydro-liquefaction of wet sewage sludge. *Bioresour Technol* 2015;187:23–9.
- [64] Shuping Z, Yulong W, Mingde Y, Kaleem I, Chun L, Tong J. Production and characterization of bio-oil from hydrothermal liquefaction of microalgae *Dunaliella tertiolecta* cake. *Energy* 2010;35(12):5406–11.
- [65] Chen WT, Zhang Y, Zhang J, Schideman L, Yu G, Zhang P, et al. Co-liquefaction of swine manure and mixed-culture algal biomass from a wastewater treatment system to produce bio-crude oil. *Appl Energy* 2014;128:209–16.